A role for Rab5 in structuring the endoplasmic reticulum

Anjon Audhya, Arshad Desai, and Karen Oegema

Ludwig Institute for Cancer Research, Department of Cellular and Molecular Medicine, University of California, San Diego, La Jolla, CA 92093

The endoplasmic reticulum (ER) is a contiguous network of interconnected membrane sheets and tubules. The ER is differentiated into distinct domains, including the peripheral ER and nuclear envelope. Inhibition of two ER proteins, Rtn4a and DP1/NogoA, was previously shown to inhibit the formation of ER tubules in vitro. We show that the formation of ER tubules in vitro also requires a Rab family GTPase. Characterization of the 29 *Caenorhabditis elegans* Rab GTPases reveals that depletion of RAB-5 phenocopies the defects in peripheral ER structure that result from depletion of RET-1 and YOP-1, the *C. elegans* homologues of Rtn4a and DP1/NogoA. Perturbation of endocytosis by other means did not affect ER structure; the role of RAB-5 in ER morphology is thus independent of its well-studied requirement for endocytosis. RAB-5 and YOP-1/RET-1 also control the kinetics of nuclear envelope disassembly, which suggests an important role for the morphology of the peripheral ER in this process.

Introduction

The ER is a single contiguous compartment (Terasaki and Jaffe, 1991; Cole et al., 1996; Terasaki, 2000) that is differentiated into at least three functionally distinct domains: rough ER, smooth ER, and nuclear envelope (Palade, 1955; Watson, 1955; Baumann and Walz, 2001). Cumulatively, these ER domains partition the nuclear contents from the cytoplasm and direct the synthesis of lipids, as well as membrane and secretory proteins (Estrada de Martin et al., 2005; Hetzer et al., 2005; Margalit et al., 2005; Shibata et al., 2006; Vedrenne and Hauri, 2006). The ER is also a signaling organelle that serves as a storage site for intracellular calcium and regulates its uptake and release into the cytoplasm (Papp et al., 2003).

Structurally, the ER network consists of membrane tubules, flattened sheets, and cisternae. The thickness of ER sheets is similar to the diameter of ER tubules, typically 60–100 nm, suggesting that common structural elements underlie these morphologically distinct forms (Shibata et al., 2006). The differing morphologies exhibited by ER domains likely contribute to their distinct functions. Rough ER, specialized for protein synthesis and folding, is often found in ribosome-studded sheets. In contrast, smooth ER, a site for lipid synthesis, contact with other organelles, and vesicle budding and fusion, lacks ribosomes and is often tubular (Baumann and Walz, 2001). The nuclear envelope, perhaps the most highly differentiated region of the ER, is a polarized sheet that regulates the movement of macromolecules between the nuclear space and the cytoplasm (Hetzer et al., 2005; Prunuske and Ullman, 2006). The membrane on one side of the sheet, the outer nuclear membrane (ONM), faces the cytoplasm, and on the opposite side of the lumen, the inner nuclear membrane (INM) faces the chromatin. Nuclear pores, gated channels between the cytoplasm and the nuclear interior, pass through both membrane bilayers and are sites where the INMs and ONMs are fused to each other (Salina et al., 2001; Hetzer et al., 2005; Tran and Wente, 2006). Resident INM proteins pass from the ONM to the INM by diffusion or active transport through the nuclear pores and concentrate in the INM as a result of interactions with the underlying chromatin and the nuclear lamina (Gerace and Burke, 1988; Soullam and Worman, 1995; Ellenberg et al., 1997; Holmer and Worman, 2001; Ohba et al., 2004; Gruenbaum et al., 2005; King et al., 2006).

Visualization in living cells has revealed the dynamic nature of the ER network. ER tubules in the periphery of mammalian cells continuously form and fuse, generating a meshwork characterized by the presence of "three-way" junctions between tubules that can move relative to one another (Lee and Chen, 1988; Waterman-Storer and Salmon, 1998; Estrada de Martin et al., 2005). The ER is also structurally reorganized during cell

Correspondence to Anjon Audhya: aaudhya@ucsd.edu; or Karen Oegema: koegema@ucsd.edu

Abbreviations used in this paper: dsRNA, double-stranded RNA; GDI, GDP-dissociation inhibitor; GEF, guanine nucleotide exchange factor; INM, inner nuclear membrane.

The online version of this article contains supplemental material.

The Journal of Cell Biology, Vol. 178, No. 1, July 2, 2007 43–56
http://www.jcb.org/cgi/doi/10.1083/jcb.200701139

cycle progression. One prominent example is in animal cells, where the nuclear envelope disassembles during mitotic entry to promote spindle assembly. After the chromosomes separate in anaphase, nuclear envelopes reform around each of the separated chromatin masses (Mattaj, 2004; Margalit et al., 2005; Prunuske and Ullman, 2006). The peripheral ER also undergoes cell cycle–dependent changes. In eggs from a variety of vertebrate and invertebrate species, there is a dramatic clustering of the peripheral ER network during mitosis (Bobinnec et al., 2003; Poteryaev et al., 2005; Stricker, 2006). This has been particularly well characterized in *Xenopus laevis* oocytes, where electron microscopy revealed the formation of "mitotic ER clusters" between 1 and 5 μm in diameter composed of packed smooth ER tubules and cisternae (Terasaki et al., 2001).

Relatively little is known about the factors that shape ER tubules and sheets, how the domains within the contiguous ER network maintain their distinct morphologies, or how transitions in the organization of the ER network during cell cycle progression are orchestrated. However, the development of systems for assembly of ER tubules from vesicles in vitro has led to some molecular insight. The reticulon family member Rtn4a was identified based on its modification by sulfhydryl reagents that inhibit the assembly of ER tubules (Voeltz et al., 2006). Inhibition of Rtn4a by antibody addition to the in vitro reaction did not block vesicle fusion but prevented the fused vesicles from adopting an elongated tubule-like morphology. These results suggest that ER tubule formation requires both homotypic vesicle fusion and factors, including Rtn4a, that confer a tubular, rather than spherical, geometry. Rtn4a interacts with a second integral membrane protein called DP1/NogoA, and in *Saccharomyces cerevisiae*, Ret1p and Yop1p, homologues of Rtn4a and DP1/NogoA, localize to the ER and play a functionally redundant role in the maintenance of peripheral ER tubules (Voeltz et al., 2006). The mechanisms that drive homotypic fusion during the assembly of ER tubules remain unclear. In vitro, fusion requires GTP and is inhibited by a nonhydrolyzable GTP analogue (Dreier and Rapoport, 2000). In addition, a previous study demonstrated that the homotypic fusion of mammalian ER microsomes could be blocked by Rab GDP-dissociation inhibitor (GDI), implicating a Rab-type GTPase in the fusion reaction (Turner et al., 1997).

Here, we use the *Caenorhabditis elegans* embryo as a model system to explore the molecular requirements for ER structure and dynamics. We show that simultaneous inhibition of YOP-1 and RET-1, the *C. elegans* homologues of DP1 and Rtn4a, results in a defect in ER morphology that is most pronounced during mitosis, when the ER is coalesced. Using this phenotype as a guide, we examined embryos depleted of each of the 29 *C. elegans* Rab family GTPases. Surprisingly, we found that specific depletion of the endosomal Rab-type GTPase, RAB-5, resulted in a defect in ER morphology that closely resembled depletion of YOP-1/RET-1. Both RAB-5 and YOP-1/RET-1 are also required for timely disassembly of the nuclear envelope during mitosis. Cumulatively, these results demonstrate a role for Rab5 in ER structure that is independent of its previously characterized functions during endocytosis and suggest that the morphology of the peripheral ER is important for nuclear envelope disassembly during mitotic entry.

Results

RET-1 and YOP-1 are redundantly required for ER morphology

To explore the molecular requirements for ER structure, we used the first division of the *C. elegans* embryo as a model system. In *C. elegans* (Poteryaev et al., 2005), as in eggs from other vertebrate and invertebrate species (Kline, 2000; Terasaki et al., 2001; Bobinnec et al., 2003), the ER coalesces during mitosis into a reticular network of thick tubules and "mitotic ER clusters." Because the interphase network of fine ER tubules is difficult to resolve at the light microscopic level, examination of the ER in its coalesced mitotic state provides a convenient means to identify defects in ER structure. We monitored ER dynamics by imaging embryos expressing a GFP fusion with the lumenal signal peptidase SP-12 (Poteryaev et al., 2005). After fertilization, the oocyte- and sperm-derived pronuclei migrate toward each other. The two pronuclei meet, and the nuclear/centrosome complex moves to the embryo center and rotates onto the long axis of the cell. Subsequently, the nuclear envelopes become permeable, and the mitotic spindle assembles (Fig. 1 A). During interphase, before pronuclear migration, GFP:SP-12 was present in the pronuclear envelopes as well as in a network of fine tubules and punctate structures dispersed throughout the cytoplasm. As the embryos entered mitosis, the ER coalesced to form a reticular network of thicker tubules and mitotic clusters (Fig. 1, B and D; and Video 1, available at http://www.jcb.org/cgi/content/full/jcb.200701139/DC1; Poteryaev et al., 2005). The clusters began to form ∼80 s before the onset of nuclear envelope disassembly and were enriched around the centrosomes and mitotic spindle (Fig. 1, B and C, 0-s time point). The first embryonic division in *C. elegans* is polarized, and mitotic ER clusters were concentrated near the cortex in the embryo anterior (Fig. 1 B, 0-s time point, cortical plane), similar to the cortical actomyosin cytoskeleton. After chromosome segregation in anaphase, the thick tubules and clusters abruptly dispersed, and nuclear envelopes re-formed around the separated chromosome masses, returning the ER to its interphase state (Video 1).

Rtn4a and its associated protein DP1/NogoA have been implicated in ER tubule assembly in vitro (Voeltz et al., 2006). We therefore characterized the localization and depletion phenotypes for their *C. elegans* homologues, RET-1 and YOP-1. Both endogenous RET-1 (Fig. 1 E) and a GFP fusion with YOP-1 (Fig. S1, A and B, available at http://www.jcb.org/cgi/content/full/jcb.200701139/DC1) localized to the ER. Like their vertebrate and yeast homologues (Voeltz et al., 2006), RET-1 and YOP-1 concentrate in the peripheral ER and are largely excluded from the nuclear envelope, where they are de-enriched relative to the luminal ER marker SP-12 (Fig. 1 E and Fig. S1 A). Consistent with their redundant functions in budding yeast, embryos depleted of YOP-1 or RET-1 alone exhibited no appreciable defects in embryo viability or ER structure (unpublished data). However, simultaneous depletion of YOP-1 and RET-1 dramatically altered ER morphology and reduced embryonic

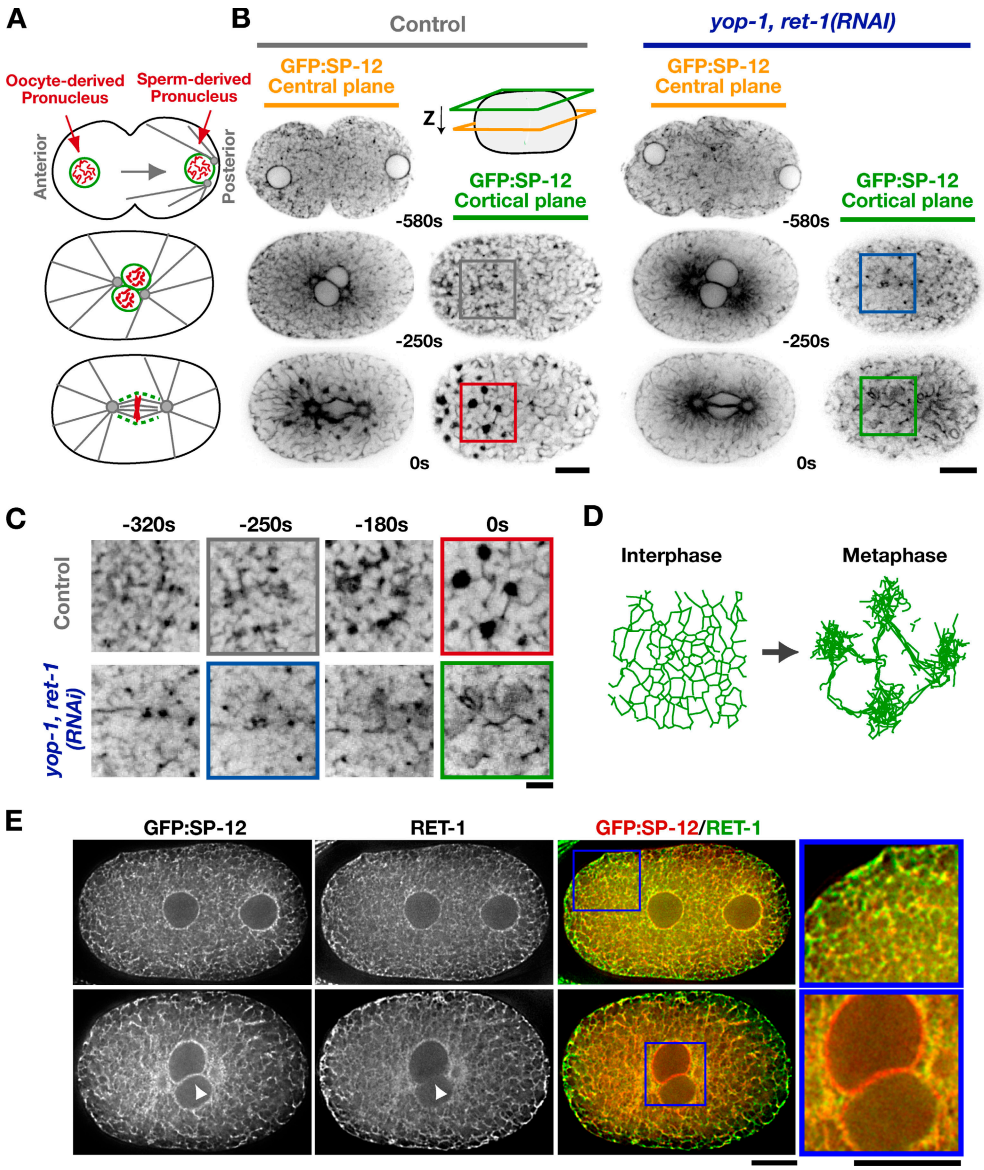

Figure 1. **RET-1 and YOP-1 are redundantly required for ER morphology.** (A) Schematics illustrate events during the first mitotic division of the *C. elegans* embryo. (B) Spinning-disk confocal optics were used to image the ER marker GFP:SP-12 in control embryos (n = 18) and embryos depleted of YOP-1 and RET-1 by RNAi (*yop-1, ret-1[RNAi]*; n = 13). Representative images of a central plane (yellow) and a cortical plane just beneath the embryo surface (green) from control (left) and *yop-1, ret-1(RNAi)* embryos (right) are shown. The time of image acquisition in seconds relative to anaphase onset is beneath the center of each image pair. Bars, 10 µm. (C) Higher magnification (2×) view of regions of each of the cortical ER panels in B. Bar, 2 µm. (D) Schematic illustrating the transition from an interphase network of thin interconnected ER tubules to a mitotic network composed of thick tubules and ER clusters. (E) Embryos expressing GFP:SP-12 fixed in early (top) and late (bottom) mitotic prophase were stained with antibodies against GFP (left) and RET-1 (middle). A single central section from a 3D computationally deconvolved image is shown for each embryo. Arrowheads point to a region of the nuclear envelope, illustrating the relative exclusion of RET-1 compared with the lumenal marker SP-12 from this ER domain. Color overlays of GFP:SP-12 (green) and RET-1 (red) and higher magnification (2.3×) views of the indicated regions (boxed) are also shown (right). Bars, 10 µm.

viability to ~40% (473 of 1191 embryos survived to hatching). The ER morphology defect was particularly evident during mitosis, when the network is normally coalesced. In YOP-1/RET-1–depleted embryos, there were fewer thick tubules that appeared shorter and more poorly organized than in control embryos, and no mitotic ER clusters were formed (Fig. 1, B and C; and Video 1). We conclude that YOP-1/RET-1 play a critical role in ER structure. In addition, their simultaneous inhibition results in a phenotype that is easily detected by monitoring ER organization in mitotic embryos using light microscopy.

Depletion of RAB-5 results in an ER morphology defect similar to YOP-1/RET-1 depletion

A visual assay for formation of a tubular ER network from salt-washed ER-enriched membranes isolated from *X. laevis* oocytes revealed that tubule assembly requires GTP, in addition to Rtn4a and DP1/NogoA (Dreier and Rapoport, 2000; Voeltz et al., 2006). To investigate the origin of this GTP requirement, we compared the ability of *X. laevis* ER-enriched membranes to form tubules after incubation with either Rab or Rho GDI, which

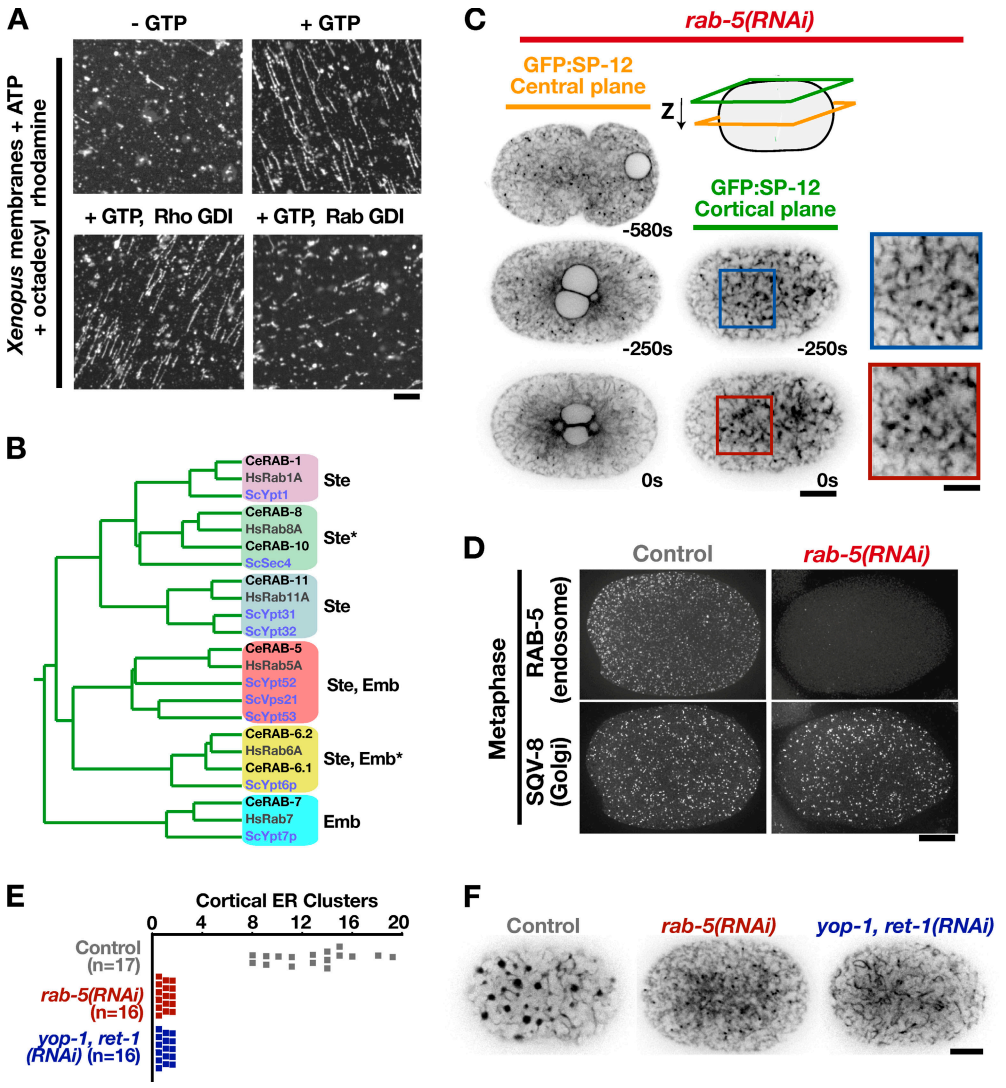

Figure 2. **Depletion of RAB-5 results in an ER morphology defect similar to depletion of YOP-1/RET-1.** (A) Salt-washed membrane vesicles isolated from *X. laevis* eggs were incubated in the absence (top left) or presence of GTP (top right) or in the presence of GTP and 30 μM Rho GDI (bottom left) or 10 μM Rab GDI (bottom right). Data are representative of four independent experiments for each condition. Bar, 5 μm. (B) A rooted phylogenetic tree based on a sequence comparison of selected Rab-type GTPases from *S. cerevisiae*, *C. elegans*, and *Homo sapiens*. Asterisks denote redundancy between RAB-8 and RAB-10 or RAB-6.1 and RAB-6.2, which must be codepleted to observe a phenotype. Lethality of the embryos produced by the dsRNA-injected mother (Emb) and/or the failure of the injected mother to produce a normal number of embryos (Ste) is indicated. (C) Spinning-disk confocal optics were used to image RAB-5–depleted embryos (*rab-5[RNAi]*; $n = 21$) expressing the ER marker GFP:SP-12, as in Fig. 1 B. Bar, 10 μm. Higher magnification (2×) views of a portion of the adjacent cortical sections are shown to the right. Bar, 5 μm. (D) Metaphase control (left) and *rab-5(RNAi)* (right) embryos were fixed and stained with antibodies to the endosome marker RAB-5 (top) and the Golgi marker SQV-8 (bottom). Images are projections of deconvolved 3D datasets. Bar, 10 μm. (E) The number of mitotic ER clusters (>0.5 μm in diameter) measured in a cortical section of embryos expressing GFP:SP-12 collected 10 s before anaphase onset is plotted for at least 16 embryos for each condition. (F) Representative cortical sections used for the quantification in E showing GFP:SP-12 in control (left), RAB-5–depleted (middle), and YOP-1– and RET-1–depleted (right) embryos 10 s before anaphase onset. Bar, 10 μm.

inhibit Rab or Rho family GTPases, respectively. Although Rho GDI failed to have any effect, addition of Rab GDI potently blocked ER tubule formation in vitro (Fig. 2 A). This result suggested that, in addition to YOP-1 and RET-1, ER structure is controlled by a Rab family GTPase.

To investigate whether a Rab GTPase contributes to ER structural dynamics in vivo, we systematically depleted each of the 29 *C. elegans* Rabs (Table S1, available at http://www.jcb.org/cgi/content/full/jcb.200701139/DC1). This analysis identified six Rab activities necessary for embryo production and/or early embryogenesis (Fig. 2 B). Of these, only reduction of RAB-5 levels resulted in an effect on ER structure similar to depletion of YOP-1/RET-1 (compare Fig. 2 C with Fig. 1, B and C; Video 1). Depletion of RAB-5, which resulted in 100% embryonic lethality, inhibited both the formation of a reticular network of thick tubules and the appearance of mitotic ER clusters (Fig. 2, C, E, and F; and Videos 1 and 2). In contrast to the dramatic effect on ER structure, staining of control and RAB-5–depleted fixed embryos with antibodies against a Golgi marker, the glucuronyltransferase SQV-8, revealed that Golgi size and distribution were not altered by RAB-5 depletion (Fig. 2 D).

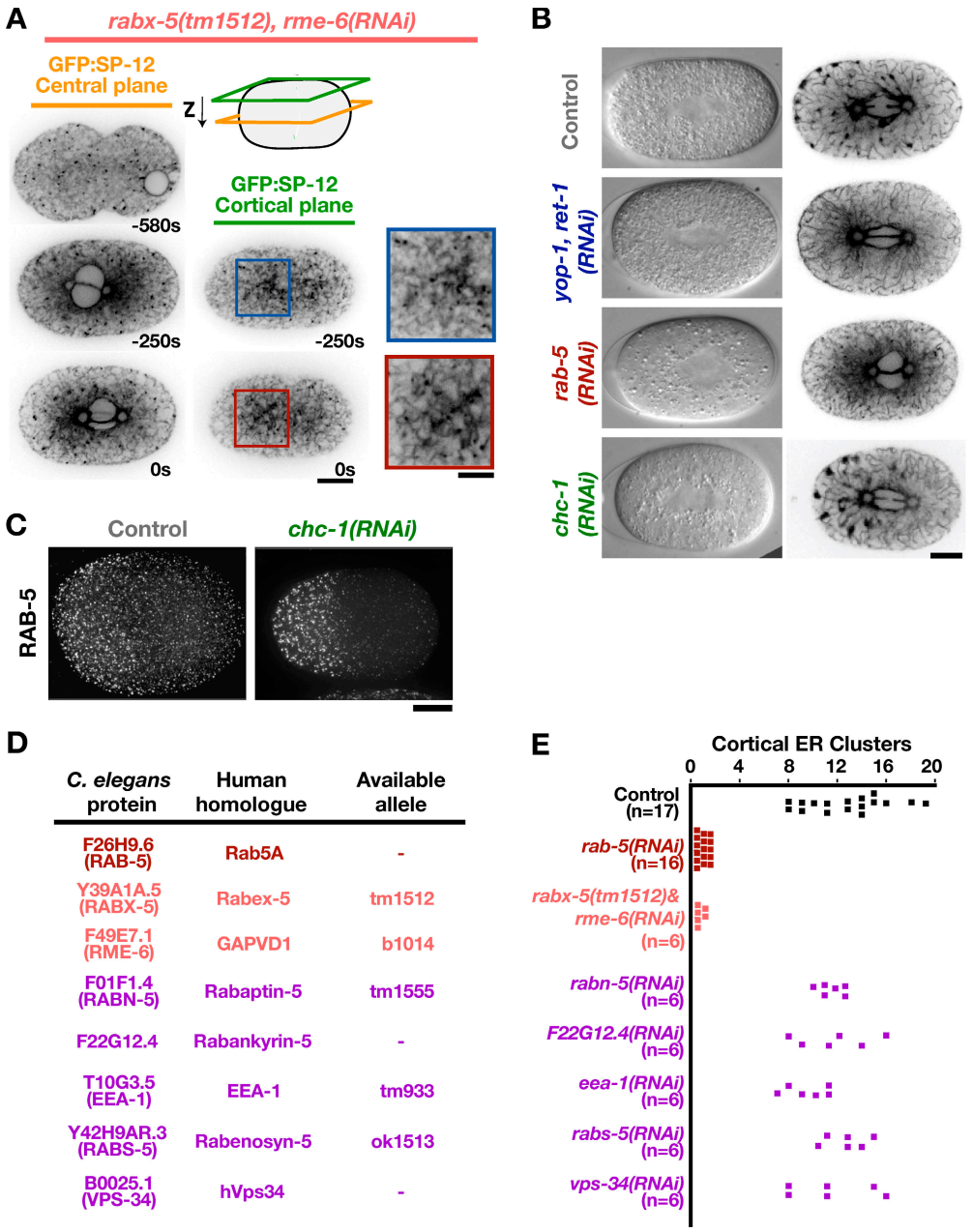

Figure 3. **RAB-5 structures the ER independently of known effectors.** (A) Spinning-disk confocal optics were used to image GFP:SP-12–expressing *rabx-5(tm1512)* mutant embryos depleted of RME-6 by RNAi (*rabx-5[tm1512], rme-6[RNAi]*; $n = 7$), as in Fig. 1 B. Bar, 10 µm. Higher magnification (2×) views of a portion of the adjacent cortical sections are shown to the right. Bar, 5 µm. (B) Differential interference contrast and spinning-disk confocal optics were used to image GFP:SP-12–expressing control ($n = 18$), *yop-1, ret-1(RNAi)* ($n = 13$), *rab-5(RNAi)* ($n = 21$), and *chc-1(RNAi)* ($n = 15$) embryos. Representative differential interference contrast (left) and GFP:SP-12 fluorescence images (right) of a single central section are shown. Bar, 10 µm. (C) Mitotic control (top) and *chc-1(RNAi)* (bottom) embryos were fixed and stained with antibodies to RAB-5. Images are projections of deconvolved 3D datasets. Bar, 10 µm. (D) A table listing the two known *C. elegans* RAB-5 GEFs (pink; Sato et al., 2005) and the *C. elegans* homologues of RAB-5 effectors (purple; Deneka et al., 2003) and their human homologues. In cases where a mutant allele was available, time-lapse sequences of living embryos from the mutant strain acquired using differential interference contrast microscopy ($n = 6$ for each condition) were analyzed for the appearance of four nuclei after the first embryonic cytokinesis, a phenotype indicative of a defect in ER structure (for details, see Fig. 5). The four-nuclei phenotype was observed when both RAB-5 GEFs were simultaneously inhibited but not in mutants for any RAB-5 effector. (E) The number of mitotic ER clusters (>0.5 µm in diameter) measured in a cortical section of embryos expressing GFP:SP-12 collected 10 s before anaphase onset is plotted for at least six embryos for each condition.

The role of RAB-5 in ER structure is independent of its requirement during endocytosis

Rab5 has an established role in endocytosis and early endosome fusion (Somsel Rodman and Wandinger-Ness, 2000; D'Hondt et al., 2000; Pfeffer, 2001; Zerial and McBride, 2001). Previous work in *C. elegans* has shown that these functions are mediated by two RAB-5 guanine nucleotide exchange factors (GEFs), RME-6 and RABX-5, which have overlapping functions (Sato et al., 2005). Examination of the ER in embryos mutant for *rabx-5* in which RME-6 was depleted by RNAi revealed a structural defect essentially identical to that in *rab-5(RNAi)* embryos

(Fig. 3, A and E), indicating that the role of RAB-5 in ER structure is also mediated by RME-6 and RABX-5.

To determine whether the effect of RAB-5 depletion on ER structure is an indirect consequence of its effect on endocytosis, we inhibited endocytosis by depleting other proteins that function in the early endocytic pathway, including clathrin heavy chain (CHC-1; Fig. 3 B), dynamin, and α-adaptin (not depicted). Depletion of CHC-1 redistributed clathrin light chain into the cytoplasm (not depicted) and resulted in a dramatic decline in cytoplasmic yolk granule density (Fig. 3 B), a hallmark of a pronounced defect in endocytosis during oocyte development (Grant and Hirsh, 1999). However, despite a reduction in yolk density similar to that in RAB-5–depleted embryos, ER morphology was not perturbed by CHC-1 depletion (Fig. 3 B). RAB-5 still localized to punctate endosomal structures in CHC-1–depleted embryos (Fig. 3 C), although the RAB-5 structures were enlarged and relatively more concentrated in the embryo anterior compared with controls. Examination of ER structure in embryos individually depleted of candidate RAB-5 effector proteins, including the *C. elegans* homologues of EEA-1, Rabenosyn-5, Rabaptin-5, and the catalytic subunit of a type 3 PI 3-kinase, hVps34 (Deneka et al., 2003), also failed to reveal any detectable alteration in ER morphology (Fig. 3, D and E).

Depletion of RAB-5 also did not substantially alter the appearance of the microtubule cytoskeleton (Fig. S1 C), which has been shown to play a role in the distribution of the ER within cells (Du et al., 2004; Vedrenne and Hauri, 2006). In addition, mitotic ER tubules and clusters still formed in nocodazole-treated embryos that lacked detectable microtubule polymer (Fig. S1 D). As previous work suggested that the actomyosin cytoskeleton also plays a role in ER structure (Poteryaev et al., 2005), we examined the distributions of GFP fusions with myosin II (GFP:NMY-2; Nance et al., 2003) and the actin binding domain of moesin (GFP:Moe), an established probe for filamentous actin in the *C. elegans* embryo (Motegi et al., 2006). In the period leading up to metaphase, the actin cytoskeleton appeared similar in control and depleted embryos (Fig. S1 E). A comparison of the distribution of GFP:NMY-2 in control, *rab-5(RNAi)*, and *chc-1(RNAi)* embryos revealed that during the establishment of polarity, the organization of cortical myosin II was also similar under all three conditions (Fig. S1 F). During mitosis, the organization of GFP:NMY-2 in *rab-5(RNAi)* embryos, although distinct from that in controls, was similar to that in the *chc-1(RNAi)* embryos (Fig. S1 G). These results suggest that although compromised endocytosis, which is common to both *rab-5(RNAi)* and *chc-1(RNAi)* embryos, does alter the organization of cortical NMY-2, this mild perturbation is not responsible for the impact of RAB-5 depletion on ER structure.

Cumulatively, these findings indicate that the defect in ER structure in RAB-5–depleted embryos is not a consequence of a general perturbation of membrane trafficking, a disruption of microtubule–ER interactions, or a defect in the organization of the actomyosin cytoskeleton, and instead support the conclusion that RAB-5 has a specific and previously unappreciated role in ER morphology.

Activated RAB-5 potentiates the formation of mitotic ER clusters

Small GTPases cycle between an active GTP-bound form and an inactive GDP-bound form. To determine whether ER structure is sensitive to activation as well as inhibition of RAB-5, we constructed transgenic strains that stably expressed $RFP^{mCherry}$ (McNally et al., 2006) fused to either wild-type RAB-5 or a mutant form of RAB-5 that dramatically slows GTP hydrolysis (Q78L). Expression of the RFP fusion with wild-type RAB-5 did not affect either endosome distribution or ER morphology (Fig. S2 A, available at http://www.jcb.org/cgi/content/full/jcb.200701139/DC1). Expression of the RFP fusion with $RAB\text{-}5^{Q78L}$, at ∼25% of the level of endogenous RAB-5 (Fig. 4 A), reduced the normal anterior bias of endosomes in the polarized one-cell embryo but did not dramatically alter endosome morphology as assessed by examination of the localization of endogenous RAB-5 (Fig. 4 B), or a GFP fusion with the endosomal marker EEA-1 (Fig. S2 F). However, expression of $RFP\text{:}RAB\text{-}5^{Q78L}$ had a striking effect on ER structure, monitored by coexpression with GFP:SP-12. More mitotic clusters that were also considerably larger than those in control embryos were observed (Fig. 4 C and Video 3). Additionally, the clusters failed to fully disperse after anaphase and often persisted into the following cell division (Video 3). Depletion of YOP-1 and RET-1 in embryos expressing $RFP\text{:}RAB\text{-}5^{Q78L}$ revealed that YOP-1 and RET-1 are required for the dramatic changes in ER structure caused by expression of the dominant-active RAB-5 mutant (Fig. 4 C). These results demonstrate that ER structure is sensitive to either depletion or activation of RAB-5, exhibiting opposing responses to the two perturbations.

Expression of mammalian $Rab5A^{Q79L}$ also potentiated the formation of mitotic ER clusters in human HeLa cells. Compared with early *C. elegans* embryos, control HeLa cells exhibited relatively few mitotic ER clusters, as did cells expressing $Rab5A^{S34N}$, a dominant-negative version of Rab5A. In contrast, expression of wild-type Rab5A resulted in a small increase, and expression of $Rab5A^{Q79L}$ resulted in a dramatic and consistent increase in the number of mitotic ER clusters >0.5 μm in diameter (Fig. S3, A and B). Cumulatively, these results suggest a conserved role for RAB-5 in controlling ER structure.

Simultaneous inhibition of RAB-5 and YOP-1/RET-1 exacerbates ER structure defects

Depletion of RAB-5 or YOP-1/RET-1 has a similar effect on ER structure. In addition, YOP-1/RET-1 are required for $RFP\text{:}RAB\text{-}5^{Q78L}$ to exert a dominant effect. These results raised the possibility that YOP-1 and RET-1 are downstream effectors of RAB-5. To determine whether YOP-1 and RET-1 are likely to be direct effectors of RAB-5, we tested whether recombinant FLAG-tagged YOP-1 or RET-1 could bind to GST:RAB-5 in vitro. However, no substantial binding of either protein to GST:RAB-5 prebound to either GDP or GTPγS was observed (Fig. S3 C). A role for YOP-1/RET-1 as downstream effectors of RAB-5 would also predict that simultaneous depletion of

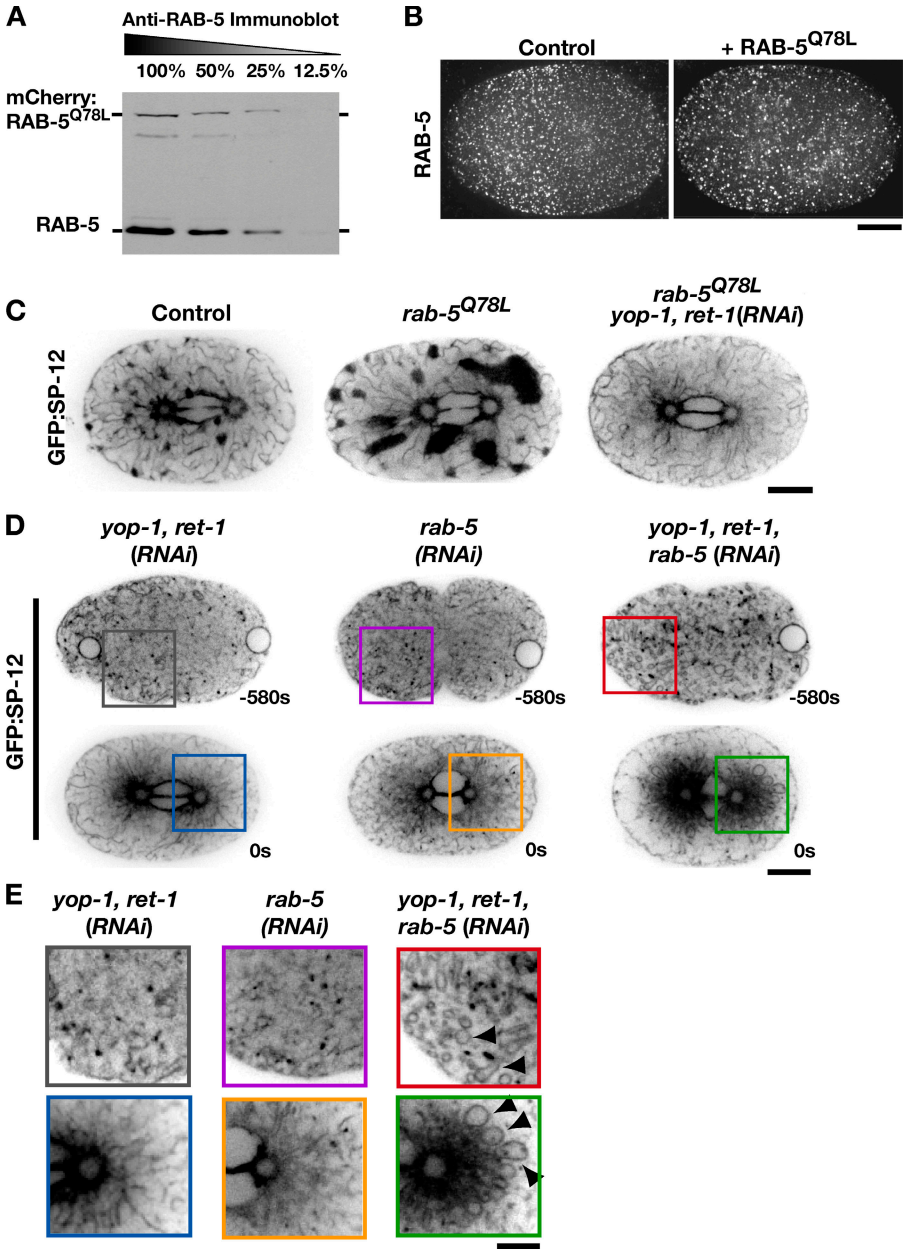

Figure 4. **Activated RAB-5 potentiates the formation of mitotic ER clusters.** (A) An anti–RAB-5 immunoblot of a serially diluted extract prepared from embryos stably expressing RAB-5^{Q78L} fused to RFP^{mCherry}. (B) Metaphase control (left) and RFP:RAB-5^{Q78L}–expressing (right) embryos were fixed and stained with antibodies to RAB-5. Projections of deconvolved 3D datasets are shown. Bar, 10 μm. (C) Embryos expressing GFP:SP-12 alone (n = 18), GFP:SP-12 and RFP:RAB-5^{Q78L} (n = 15), or GFP:SP-12 and RFP:RAB-5^{Q78L} that were also depleted of YOP-1 and RET-1 by RNAi (n = 11) were imaged using spinning-disk confocal optics. Representative images of a central plane are shown. Bar, 10 μm. (D) Embryos expressing GFP:SP-12 that were depleted of YOP-1 and RET-1 (n = 13); RAB-5 (n = 21); or YOP-1, RET-1, and RAB-5 (n = 10) were imaged by spinning-disc confocal microscopy. Representative images of a single central section are shown. Bar, 10 μm. (E) Higher magnification (2×) views of a portion of the images in D. Arrowheads highlight aberrant ER loops present during interphase and mitosis in the triple-depleted embryos. Bar, 5 μm.

YOP-1/RET-1 would not enhance the effect of RAB-5 depletion on ER morphology. However, simultaneous depletion of YOP- 1/RET-1 with RAB-5 resulted in a dramatic synergistic defect evident throughout the cell cycle (Fig. 4, D and E). In the triple-depleted embryos, ER morphology was aberrant in interphase, when GFP:SP-12 was present in numerous loop-shaped structures. These ER loops accumulated around the spindle poles as the triple-depleted embryos entered mitosis, leaving the embryo periphery nearly devoid of ER (Fig. 4 D). In addition, as in the individual depletions, the ER failed to coalesce into a network of thick tubules and clusters (Fig. 4 D and Video 4, available at http://www.jcb.org/cgi/content/full/jcb.200701139/DC1). Although it is possible that RAB-5 and YOP-1/RET-1 are on a single pathway and the synergistic defect in ER structure is due to a greater effectiveness in inhibiting this pathway when two of its constituents are depleted by RNAi, we favor the idea that the strong synergistic phenotype indicates that RAB-5 and YOP-1/RET-1 make distinct essential contributions to ER structure. It is worth pointing out, however, that the idea that RAB-5 and YOP-1/RET-1 each retain some function when the other is absent does not rule out the possibility that RAB-5 exerts its effect in part by altering the function of YOP-1/RET-1.

Both RAB-5 and YOP-1/RET-1 promote nuclear envelope disassembly

The ER is a single contiguous compartment that includes the nuclear envelope. We were therefore interested in whether, in addition to the peripheral ER, inhibition of RAB-5 or YOP-1/RET-1 altered nuclear envelope dynamics. One clue that this might be the case came from the observation that depletion of either RAB-5 or YOP-1/RET-1 resulted in a characteristic

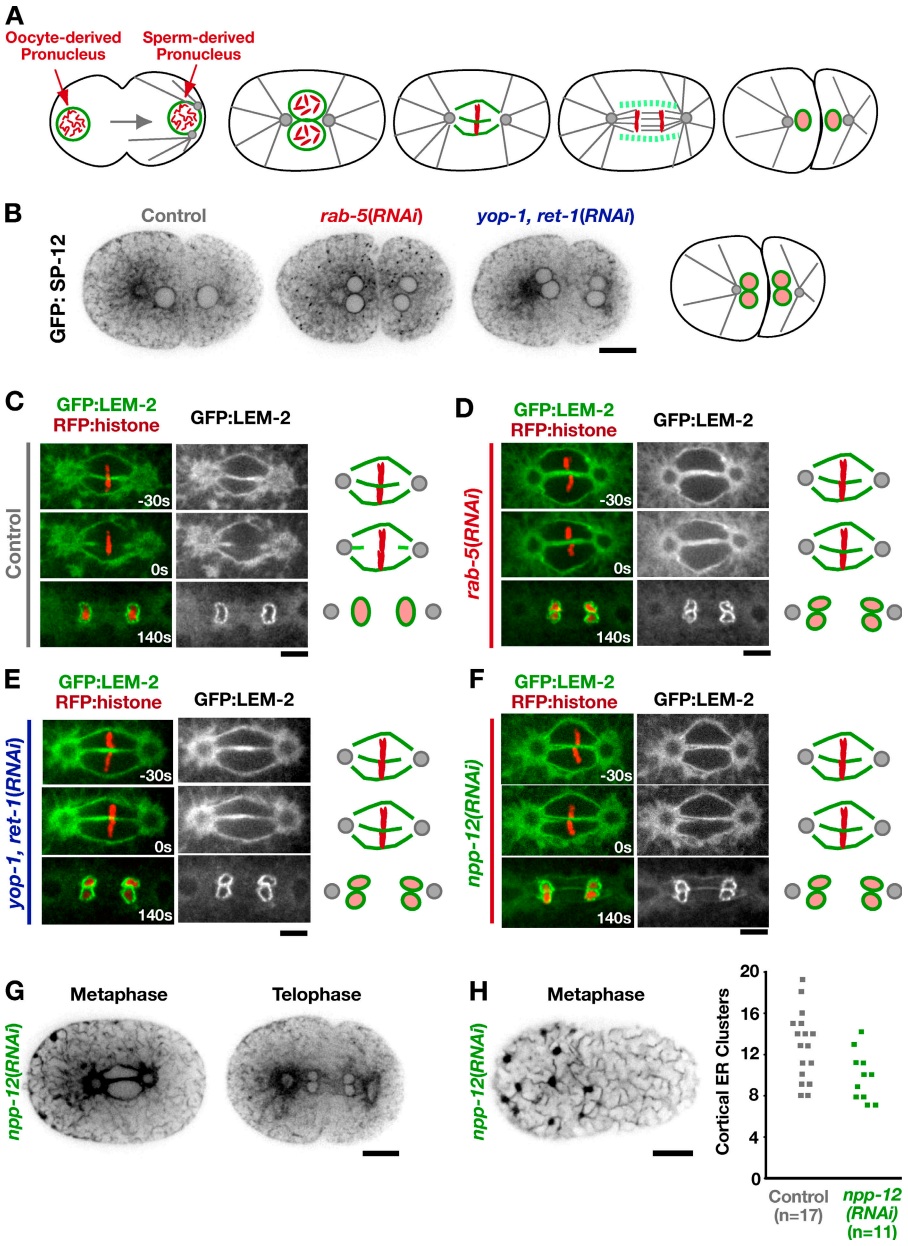

Figure 5. **RAB-5 and YOP-1/RET-1 promote nuclear envelope disassembly during mitosis.** (A) Schematics highlighting the dynamics of the oocyte- and sperm-derived pronuclear envelopes (green) during the first division of the *C. elegans* embryo. (B) Spinning-disk confocal optics were used to image control (n = 8), *rab-5(RNAi)* (n = 16), and *yop-1, ret-1(RNAi)* (n = 12) embryos expressing GFP:SP-12. A representative central section immediately after the first embryonic cytokinesis is shown. Bar, 10 μm. (C–F) Spinning-disk confocal optics were used to image control (n = 9), *rab-5(RNAi)* (n = 11), *yop-1, ret-1(RNAi)* (n = 10), and *npp-12(RNAi)* (n = 10) embryos co-expressing RFP:histone and a GFP fusion with the resident INM protein LEM-2. Representative central sections are shown. Times are in seconds relative to anaphase onset. Schematics summarize nuclear envelope dynamics under each condition. Bars, 5 μm. (G) Representative central sections of *npp-12(RNAi)* embryos expressing GFP:SP-12 during metaphase and telophase. Bar, 10 μm. (H) A representative cortical section of an *npp-12(RNAi)* embryo expressing GFP:SP-12 10 s before anaphase onset (left). Bar, 10 μm. Mitotic ER clusters were quantified as in Fig. 3 E (right).

"four-eyes" phenotype at the end of the first division, in which two nuclei instead of one re-formed in each daughter cell. In the *C. elegans* zygote, after the two pronuclei meet, the nuclear envelopes are permeabilized and cleared from the region near the centrosomes, allowing spindle microtubules to interact with and align chromosomes before their segregation (Fig. 5 A; Oegema and Hyman, 2005). After anaphase chromosome segregation, a single nuclear envelope reforms around each of the separated chromatin masses, thereby mixing the haploid sperm and oocyte genomes. In embryos in which either RAB-5 or YOP-1/RET-1 was depleted, separate nuclear envelopes formed around the sperm- and oocyte-derived chromosomes after their segregation, resulting in two nuclei in each daughter cell (Fig. 5 B).

To understand the basis for this phenotype, we filmed embryos coexpressing a GFP fusion with the INM protein LEM-2 and an $RFP^{mCherry}$ fusion with histone H2B. This analysis revealed that ~35 s before anaphase onset, the juxtaposed oocyte and sperm pronuclear envelopes in control embryos undergo a scission event in close proximity to the aligned chromosomes and are cleared from the region between the chromosomes, allowing the chromosomes from the two pronuclei to mix and form a single nucleus after segregation (Fig. 5 C and Video 5, left, available at http://www.jcb.org/cgi/content/full/jcb.200701139/DC1). In embryos in which either RAB-5 or YOP-1/RET-1 were depleted, this scission event never occurred, and the oocyte- and sperm-derived chromosomes remained separate during their segregation on the spindle (Fig. 5, D and E; and Video 5, right). Consequently, two nuclei were formed in each daughter cell, and the mixing of the genomes derived from the two gametes failed.

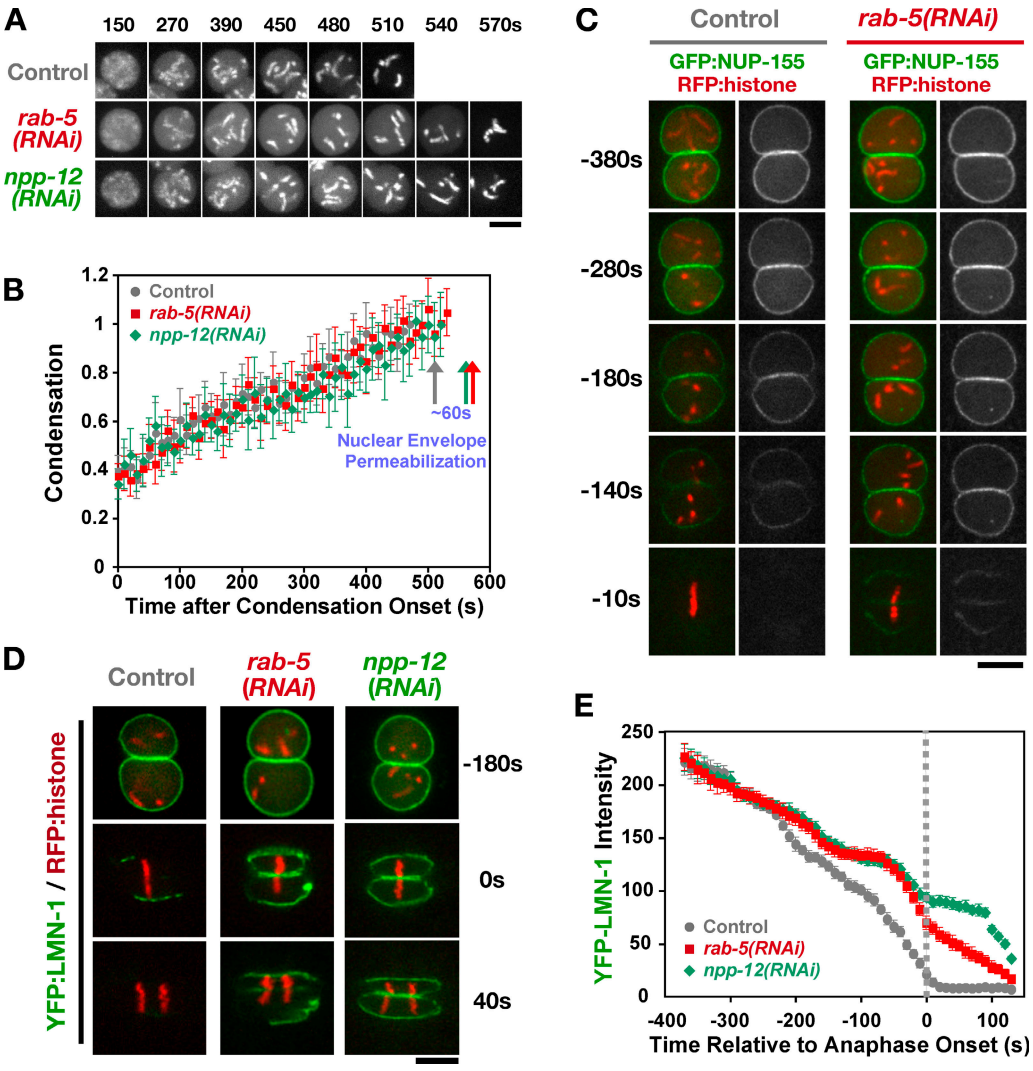

Figure 6. **RAB-5 depletion delays nuclear envelope permeabilization, nuclear pore removal, and lamina disassembly.** (A) Time-lapse spinning-disk confocal sequences of control, *rab-5(RNAi)*, and *npp-12(RNAi)* embryos expressing GFP:histone were used to measure the timing of nuclear envelope breakdown relative to chromosome condensation. Representative sequences of individual nuclei are shown. Times are with respect to condensation onset. Bar, 5 μm. (B) Plot of the mean value of the condensation parameter versus time for control (gray circles; $n = 5$), *rab-5(RNAi)* (red squares; $n = 5$), and *npp-12(RNAi)* (green diamonds; $n = 5$) embryos. Traces are displayed with the onset of condensation as t = 0. Arrows mark the timing of nuclear envelope permeabilization for each dataset. Error bars indicate SEM. (C and D) Time-lapse sequences of control and *rab-5(RNAi)* embryos expressing RFP:histone and either GFP:NUP-155 (C) or YFP:LMN-1 (D) were acquired using spinning-disk confocal optics ($n = 5$ for each condition). Images from representative sequences are shown for control (left) and *rab-5(RNAi)* (right) embryos. Times are in seconds relative to the onset of chromosome segregation. Bar, 5 μm. (E) The total fluorescence intensity of nuclear LMN-1 was measured at each time point for control ($n = 7$), *rab-5(RNAi)* ($n = 6$), and *npp-12(RNAi)* ($n = 6$) embryos. The mean value for this measurement is plotted versus time. Error bars indicate SEM. Sequences were time aligned with respect to onset of anaphase chromosome segregation.

Depletion of NPP-12 phenocopies the nuclear envelope disassembly defect resulting from RAB-5 or YOP-1/RET-1 depletion without disrupting peripheral ER structure

The four-eyes phenotype observed in YOP-1/RET-1– or RAB-5–depleted embryos is highly unusual. Functional genomic analysis of cell division in *C. elegans* identified only one other protein, the nuclear pore component NPP-12, whose depletion reproducibly results in this phenotype (Sönnichsen et al., 2005). NPP-12 is the *C. elegans* homologue of gp210, one of two integral membrane proteins associated with the nuclear pore (Holaska et al., 2002; Hetzer et al., 2005). Imaging of embryos coexpressing GFP:LEM-2 and RFP:histone confirmed that depletion of NPP-12 results in a defect in nuclear envelope disassembly similar to that resulting from depletion of RAB-5 or YOP-1/RET-1 (Fig. 5 F). However, analysis of GFP:SP-12 indicated that, in contrast to depletion of YOP-1/RET-1 or RAB-5, depletion of NPP-12 does not noticeably perturb peripheral ER structure (Fig. 5, G and H). These results indicate that the defect in nuclear envelope disassembly in the YOP-1/RET-1– and RAB-5–depleted embryos is likely to be a consequence rather than a cause of the defect in ER structure. They also point to an interesting functional connection between the role of peripheral ER structure in nuclear envelope disassembly and events occurring at nuclear pores.

Depletion of RAB-5 or NPP-12 delays multiple steps in nuclear envelope disassembly

Diffusion of membrane proteins between the peripheral ER and INM is proposed to require energy-dependent restructuring that creates transient channels through the nuclear pore membrane (Ohba et al., 2004). Antibodies to gp210 inhibit diffusion between the peripheral ER and INM, suggesting that gp210 plays a role in this restructuring (Ohba et al., 2004). A role in promoting the diffusion of integral membrane proteins between the peripheral ER and INM would provide a plausible explanation for why perturbing gp210 or peripheral ER structure has a similar effect on nuclear envelope disassembly. To explore the phenotypic similarity of these two very different perturbations further, we used a series of assays to compare nuclear envelope disassembly in NPP-12– and RAB-5–depleted embryos. Nuclear envelope disassembly is accompanied by several distinct events: (1) loss of the peripheral pore components, which renders the nuclear envelope permeable to macromolecules of progressively larger diameter (Terasaki et al., 2001; Lenart et al., 2003); (2) removal of pores from the membrane; (3) disassembly of the nuclear lamina; and (4) release of resident INM proteins back into the peripheral ER (Hetzer et al., 2005; Prunuske and Ullman, 2006). Because the dependencies between these different events are not clear, we compared the effects of RAB-5 and NPP-12 depletion on all of them.

To determine if nuclear envelope permeabilization was affected, we filmed embryos expressing GFP:histone H2B and measured the timing of nuclear envelope permeabilization with respect to the kinetics of chromosome condensation. Permeabilization was followed by monitoring the diffusion of free GFP:histone out of the nucleus, which occurs within 60 s of the entry of cytoplasmic 70-kD dextran into the nucleus (Portier et al., 2007). We refer to the time point when the free nuclear GFP:histone fluorescence has equilibrated with the cytoplasm as nuclear envelope permeabilization. To analyze chromosome condensation, we used a recently developed image analysis method that can be used to quantitatively compare condensation kinetics between control and specifically perturbed embryos (Maddox et al., 2006). This analysis revealed that the kinetics of chromosome condensation were not altered by depletion of either RAB-5 or NPP-12. However, both perturbations resulted in a 50–60-s delay between the completion of chromosome condensation and nuclear envelope permeabilization (Fig. 6, A and B). Timing the release of a NLS-containing GFP fusion protein (GFP-LacI) from the nucleus relative to anaphase onset provided independent support that permeabilization is delayed by ∼50 s in RAB-5–depleted embryos (Fig. S4, A–C, available at http://www.jcb.org/cgi/content/full/jcb.200701139/DC1).

To analyze the removal of nuclear pores from the envelope, we filmed embryos expressing a GFP fusion with NUP-155, a stable component of the pore wall (Franz et al., 2005). Redistribution of NUP-155 from the nuclear rim to the cytoplasm was delayed by ∼50 s in RAB-5– and NPP-12–depleted embryos (Fig. 6 C and not depicted). Disassembly of the nuclear lamina was also similarly delayed by both perturbations. Although a YFP fusion with the *C. elegans* B-type lamin LMN-1 is nearly completely removed from the nuclear envelope by anaphase onset in control embryos, substantial amounts of LMN-1 remained at anaphase onset in RAB-5– or NPP-12–depleted embryos (Fig. 6 D). Fluorescence intensity measurements revealed that until anaphase onset, lamin disassembly is quantitatively similar between RAB-5– and NPP-12–depleted embryos (Fig. 6 E).

We next investigated the effect of depletion of RAB-5 and NPP-12 on the release of resident INM proteins into the peripheral ER. In the *C. elegans* embryo, the INM protein LEM-2 is present in the peripheral ER throughout the cell cycle. As the nuclear envelope forms in telophase, LEM-2 becomes selectively enriched in this ER domain (Fig. S4 E). Because the presence of LEM-2 in ER concentrated around mitotic spindle poles interfered with visualization of LEM-2 associated with the nuclear envelope, we examined the effect of RAB-5 depletion in *spd-5*(RNAi) embryos, which lack functional centrosomes and fail to build mitotic spindles (Fig. 7 A). In embryos depleted of SPD-5 alone, the peripheral ER exhibits normal dynamics and is coalesced during mitosis to form a network of thick tubules and clusters (Fig. 7 B). As expected, when both SPD-5 and RAB-5 were depleted, there was a profound defect in the formation of thick tubules and clusters during mitosis (Fig. 7 B). In embryos depleted of SPD-5 alone, LEM-2 is completely dispersed into the surrounding ER and then reaccumulates around the chromatin as it begins to decondense. In contrast, in embryos codepleted of either RAB-5 or NPP-12 with SPD-5, the redistribution of LEM-2 failed to occur (Fig. 7, C–E).

Cumulatively, these results indicate that depletion of RAB-5 or NPP-12 results in a similar, broadly based defect in nuclear envelope disassembly, in which the release of INM proteins into the peripheral ER is blocked and nuclear envelope permeabilization, pore removal, and lamina disassembly are delayed. These results highlight a central importance of peripheral ER structure in ensuring timely nuclear envelope disassembly.

Discussion

A role for Rab5, the canonical endocytic Rab GTPase, in ER structure

Here, we show that ER morphology is sensitive to both depletion and activation of RAB-5, exhibiting opposing responses to the two perturbations. The effect of RAB-5 depletion on ER structure phenocopies the depletion of YOP-1/RET-1, two ER proteins previously implicated in the assembly of ER tubules in vitro. Experiments in human cells expressing a dominant-active mutant form of Rab5A suggest that the role of Rab5 in controlling ER structure is likely to be conserved. We discuss the nature of the defects in peripheral ER structure and nuclear envelope disassembly observed in RAB-5– and YOP-1/RET-1–depleted embryos and speculate on underlying mechanisms.

The defects in ER morphology in RAB-5– and YOP-1/RET-1–depleted embryos are most prominent during mitosis and could therefore reflect a specific role for RAB-5 and YOP-1/RET-1 in restructuring the interphase peripheral ER network during mitotic entry. Alternatively, YOP-1/RET-1 and RAB-5 may be required to maintain a normal ER network during interphase,

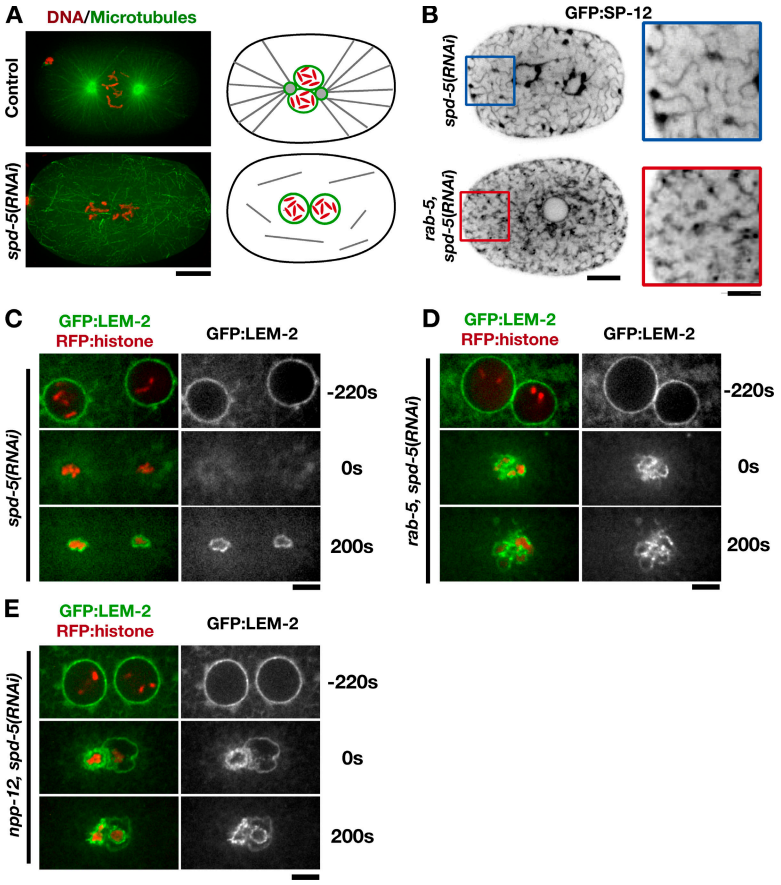

Figure 7. **Depletion of RAB-5 prevents the mitotic redistribution of INM proteins.** (A) Mitotic control (top) and *spd-5(RNAi)* (bottom) embryos were fixed and stained for DNA (red) and microtubules (green). Projections of deconvolved 3D datasets are shown. Centrosomes are absent in *spd-5(RNAi)* embryos; schematics to the right illustrate the organization of the microtubule cytoskeleton under both conditions. Bar, 10 μm. (B) Embryos expressing GFP:SP-12 were imaged using spinning-disk confocal microscopy after depletion of SPD-5 alone ($n = 7$) or both SPD-5 and RAB-5 ($n = 6$). Representative central plane images of mitotic embryos are shown. Bar, 10 μm. Higher magnification (2×) panels are shown on the right. Bar, 5 μm. (C–E) Time-lapse sequences of embryos coexpressing RFP:histone and GFP:LEM-2 depleted of SPD-5 alone (C), SPD-5 and RAB-5 (D), or SPD-5 and NPP-12 (E) were acquired using spinning-disk confocal optics ($n = 5$ for each condition). Selected images from representative sequences are shown. Sequences were aligned based on the timing of chromosome decondensation (0 s). Bars, 5 μm.

which is then the substrate for mitotic coalescence. We favor the later possibility for three reasons. First, in embryos that are simultaneously depleted of YOP-1/RET-1 and RAB-5, obvious defects in ER structure are apparent in interphase (Fig. 4, D and E). Second, reticulon/Rab-dependent assembly of ER tubules in vitro from *X. laevis* oocyte membranes is inhibited by mitotic but not interphase cytosol (Dreier and Rapoport, 2000). Third, defects in ER structure are apparent when Yop1p and the reticulons are deleted in budding yeast, regardless of cell cycle state (De Craene et al., 2006; Voeltz et al., 2006).

Previous work has identified >20 different effectors that link Rab5 to a variety of cellular activities (Christoforidis et al., 1999). However, technical difficulties have prevented the isolation of integral membrane proteins that respond to Rab5 signaling. The fact that depletion of YOP-1/RET-1 has an effect on ER structure that is similar to that of depletion of RAB-5, and the requirement for YOP-1/RET-1 for RFP:RAB-5^{Q78L} to exert a dominant effect, make YOP-1 and RET-1 attractive candidates for integral membrane effectors that link RAB-5 to the ER. Interestingly, the budding yeast homologue of YOP-1, Yop1p, was identified based on the fact that a short amino acid stretch in its N terminus interacts with Yip1, a protein implicated in the dissociation of Rab GTPases from GDI. In addition, Yop1p was found to interact with multiple Rab-type GTPases in yeast, potentially via their prenylation motifs (Calero et al., 2001). Although a conventional in vitro approach using GST:RAB-5 isolated from bacteria failed to uncover evidence for a direct interaction between RAB-5 and either YOP-1 or RET-1 (Fig. S3 C), it is possible that this interaction requires prenylation of RAB-5 and/or membrane association of YOP-1/RET-1, and hence a different approach may be needed to uncover an interaction. In addition to YOP-1 and RET-1, our data suggest the existence of additional effectors, as simultaneous depletion of RAB-5 exacerbates the defect in ER morphology present in embryos depleted of YOP-1/RET-1 alone (Fig. 4, D and E). A combination of genetic analysis in *C. elegans* with in vitro biochemical reconstitution of ER tubules using *X. laevis* membranes will likely be useful to uncover these important factors.

Control of ER structure by trans-acting small GTPases—an emerging theme?

RAB-5 was the only Rab GTPase whose depletion phenocopied the effect of YOP-1/RET-1 depletion on ER structure. This finding was surprising because RAB-5 localizes to endosomes and has well-studied functions in endocytosis and early endosome fusion (for reviews see D'Hondt et al., 2000; Somsel Rodman and Wandinger-Ness, 2000; Pfeffer, 2001; Zerial and McBride, 2001). Inhibition of endocytosis by other means, such as CHC-1 depletion, does not affect ER structure but also does not abolish localization of RAB-5 (Fig. 3 C), indicating that endosomes, although abnormal, are still present. In contrast to CHC-1 depletion, simultaneous inhibition of the two characterized RAB-5 GEFs, RME-6 and RABX-5, redistributes RAB-5 to the cytoplasm (Sato et al., 2005) and phenocopies the effect of RAB-5 depletion (Fig. 3, A and E). These results suggest that endosomal RAB-5 acts in trans to control ER structure.

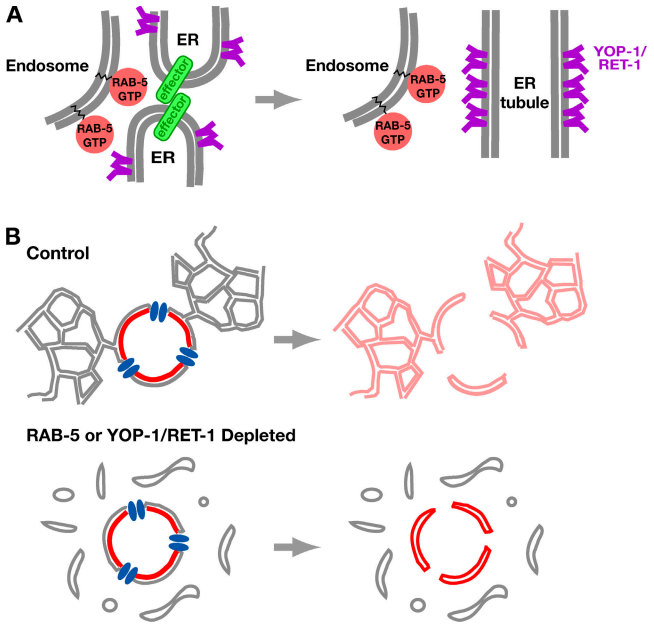

Figure 8. **A model for the role of RAB-5 in ER structure.** (A) In this model, RAB-5 on endosomes interacts with effectors on ER membranes in trans to promote their homotypic fusion. Tubule formation also requires YOP-1 and RET-1, integral ER membrane proteins that serve a structural role. (B) A model for the role of peripheral ER morphology in nuclear envelope breakdown. During nuclear envelope breakdown, the peripheral ER promotes nuclear envelope disassembly by acting as a sink for the diffusion of components of the INM (red) after their release from chromatin and the nuclear lamina. When ER morphology is disrupted by depletion of RAB-5 or YOP-1/RET-1, the diffusion to the peripheral ER is inhibited and the nuclear envelope fails to fully disassemble.

Consistent with this idea, ER tubule assembly in vitro does not require ongoing endocytosis but does require the function of a Rab-type GTPase.

We propose that active RAB-5 on endosomes transiently interacts with effectors on ER membranes to promote their homotypic fusion (Fig. 8 A). Consistent with the idea that interactions with endosomes might alter ER structure, the ER has also been shown to contact several other organelles, including the Golgi, plasma membrane, lysosomes, and late endosomes (Voeltz et al., 2002). In the one-cell embryo, the asymmetric clustering of the ER also mirrors the asymmetric distribution of endosomes (Fig. S2 A), consistent with a trans-acting mechanism. The hypothesis that RAB-5 acts in trans to control ER structure is similar to the proposal that the small GTPase Ran, together with chromatin, promotes the homotypic fusion of ER membranes to form the nuclear envelope (Hetzer et al., 2000). In this case, a chromatin-activated small GTPase signals in trans to promote ER membrane fusion. Depletion of RAB-5 does not prevent nuclear envelope assembly, and depletion of RAN-1 does not disrupt ER structure (unpublished data), indicating that these two reactions, which both require fusion of ER membranes, depend on signaling from distinct small GTPases. Another instance in which ER structural changes might be triggered by signals presented in trans is during autophagy, when a double-membrane layer that may be derived from ER membranes forms around a portion of the cytoplasm to create an autophagosome (Dunn, 1990; Klionsky and Emr, 2000). Interestingly, recent work suggests a role for the Rab24 GTPase during starvation-induced autophagy, although its precise function in this process remains unknown (Munafo and Colombo, 2002). Why would ER structure be controlled by trans-acting GTPases? One possibility is that trans-action restricts homotypic ER fusion to specific times and places within the cell to facilitate the formation of a network or envelope as opposed to large membrane aggregates.

A connection between peripheral ER morphology and nuclear envelope disassembly

We show that depletion of YOP-1/RET-1 or RAB-5 leads to a defect in nuclear envelope disassembly in addition to disrupting the morphology of the peripheral ER. Further characterization of this defect revealed a striking phenotypic similarity to depletion of NPP-12, the *C. elegans* homologue of the nuclear pore-associated integral membrane protein, gp210. Although both perturbations delay nuclear envelope permeabilization, pore removal, and lamina disassembly, the most pronounced consequence of either depletion is an essentially complete block in the release of INM components into the peripheral ER.

RAB-5 and YOP-1/RET-1 may directly restructure the nuclear envelope in addition to the peripheral ER. However, we suspect that the contribution of RAB-5 and YOP-1/RET-1 to nuclear envelope disassembly occurs indirectly via their function in structuring the peripheral ER. Consistent with this idea, YOP-1/RET-1 and their homologues in other organisms are selectively enriched in the peripheral ER relative to the nuclear envelope (Fig. 1 E; Fig. S1 A; Voeltz et al., 2006). Previous work has shown that INM components disperse into the peripheral ER during mitosis after their release from chromatin and the nuclear lamina (Yang et al., 1997; Mattaj, 2004). We therefore propose that disruption of peripheral ER morphology in RAB-5– and YOP-1/RET-1–depleted embryos prevents the diffusion of INM proteins, trapping them in the spindle region (Fig. 8 B). In this context, the fact that depletion of NPP-12/gp210 phenocopies the effect of disruption of the peripheral ER on nuclear envelope disassembly would support the previous suggestion that NPP-12/gp210 acts as a gatekeeper that positively regulates the diffusion of membrane proteins between the INM and peripheral ER (Ohba et al., 2004). We would like to emphasize that although depletion of RAB-5 or YOP-1/RET-1 results in defects in both mitotic clustering of the peripheral ER and in nuclear envelope breakdown, our data do not demonstrate that these phenotypes are linked (i.e., cluster formation stimulates nuclear envelope breakdown). It remains equally likely that these two phenotypes are independent consequences of disruption of peripheral ER structure.

In summary, our results suggest that trans-acting mechanisms involving small GTPases play an integral role in structuring the distinct domains, including the peripheral ER and nuclear envelope, within the contiguous ER network. In addition to identifying a new role for Rab5 in ER structure, our analysis also supports a role for peripheral ER structure in nuclear envelope disassembly.

Materials and methods

Worm strains and DNA manipulations

The generation of *C. elegans* strains expressing fluorescent fusions with histone H2B (Oegema et al., 2001), LEM-2 (Galy et al., 2003), LMN-1 (Galy et al., 2003), SP-12 (Poteryaev et al., 2005), and NUP-155 (Franz et al., 2005) has been described previously. Other fluorescent fusions with YOP-1 (Y71F9B.3), RAB-5 (F26H9.6), and SP-12 (C34B2.10) were generated by cloning the unspliced genomic loci into the SpeI sites of pIC26 (GFP; Cheeseman et al., 2004) or pAA64 ($RFP^{mCherry}$; McNally et al., 2006). The activated form of RAB-5 (Q78L) was generated by subjecting the spliced genomic locus of F26H9.6 to site-directed mutagenesis before cloning into pAA64. Constructs were integrated into DP38 (*unc-119* (*ed3*)) as described previously (Praitis et al., 2001) using a particle delivery system (Biolistic PDS-1000/He; Bio-Rad Laboratories, Inc.). All strains used in this study are listed in Table S2 (available at http://www.jcb.org/cgi/content/full/jcb.200701139/DC1). The strains expressing GFP:2xFYVE and GFP:NUP-155 were provided by B. Grant (Rutgers University, Piscataway, NJ) and P. Askjaer (Parc Científic de Barcelona, Barcelona, Spain), respectively.

RNA-mediated interference and antibody production

Double-stranded RNA (dsRNA) was prepared as described previously (Oegema et al., 2001) from templates prepared by using the primers listed in Table S3 (available at http://www.jcb.org/cgi/content/full/jcb.200701139/DC1) to amplify N2 genomic DNA. For complete and partial depletions, L4 hermaphrodites were injected with dsRNA and incubated at 20°C for 45 or 22–24 h, respectively, before analysis. Antibodies against RAB-5 and RET-1 were generated by cloning nucleotides 124–612 of F26H9.6 (RAB-5) and the entire coding sequence of W06A7.3b (RET-1), amplified from a cDNA library, into pGEX6P-1 (GE Healthcare). Purified GST fusion proteins were outsourced for injection into rabbits (Covance). Both antibodies were affinity purified from serum as described previously (Desai et al., 2003) by binding to columns of the same antigen after removal of the GST tag by cleavage with PreScission protease. Antibodies directed against SQV-8 and GFP have been described previously (Audhya et al., 2005; Sato et al., 2006).

Microscopy and condensation analysis

For analysis of fixed embryos, images were acquired using a 100×, 1.35 NA U-Planapo oil-objective lens (Olympus) mounted on a DeltaVision microscope system (Applied Precision) equipped with an Olympus IX70 base and a charge-coupled device camera (CoolSnap; Roper Scientific). Immunofluorescence of fixed embryos was performed as described previously (Desai et al., 2003), using the following rabbit antibodies at a concentration of 1 μg/ml: α-RAB-5 (Cy3 labeled), the mouse monoclonal antibody DM1α (Oregon green 488 labeled; Sigma-Aldrich), α-SQV-8 (Cy-5 labeled), and the goat polyclonal GFP antibody (Oregon green 488 labeled). For live analysis, embryos were mounted as described previously (Oegema et al., 2001) and imaged at 20°C on a spinning-disc confocal microscope (Eclipse TE2000-E; Nikon) equipped with a Nikon 60×, 1.4 NA Planapo oil-objective lens and a charge-coupled device camera (Orca-ER; Hamamatsu). To depolymerize microtubules, meiotic embryos were dissected directly into meiosis media (25 mM Hepes, pH 7.4, 60% Leibowitz L-15 Media, 20% fetal bovine serum, and 500 μg/ml inulin) containing 10 μg/ml nocodazole and imaged in a depression slide sealed with petroleum jelly. Quantification of ER cluster formation and lamin and LacI fluorescence intensity measurements were performed using MetaMorph software. Analysis of chromosome condensation was performed as described previously (Maddox et al., 2006). The mean value of the condensation parameter was calculated after aligning the image sequences with respect to nuclear envelope permeabilization. To simplify presentation, the plots of the condensation parameters are displayed aligned with respect to the onset of condensation.

In vitro ER tubule assembly

A light membrane fraction from *X. laevis* egg extracts was prepared as described previously (Voeltz et al., 2006), stained with octadecyl rhodamine, and mounted on glass slides to visualize tubule formation. To test the effect of GDI addition, membranes were preincubated for 10 min with either 10 μM Rab GDI or 30 μM Rho GDI, followed by the addition of 1 mM ATP and 0.5 mM GTP. Reactions were allowed to proceed for 60 min before staining and pipette transfer onto slides. Purified Rho GDI was provided by G. Bokoch (The Scripps Research Institute, La Jolla, CA), and the construct to express Rab GDI was a gift from W. Balch (The Scripps Research Institute).

Online supplemental material

Fig. S1 shows that YOP-1 localizes to the ER and nuclear envelope, reorganization of the ER during mitosis does not require microtubules, and the defect in ER organization observed after RAB-5 depletion is not caused by a perturbation in the actomyosin cytoskeleton. Fig. S2 shows that RAB-5–containing early endosomes contact the ER more frequently than RAB-7–containing late endosomes, and EEA-1 localization is lost after RAB-5 depletion but only subtly perturbed upon $RAB\text{-}5^{Q78L}$ expression. Fig. S3 shows that $Rab5A^{Q79L}$ overexpression potentiates ER cluster formation in HeLa cells, and neither YOP-1 nor RET-1 binds to GTP-loaded GST:RAB-5. Fig. S4 shows that nuclear envelope permeabilization is delayed in embryos depleted of RAB-5, GFP:2xFYVE does not localize to the nuclear envelope, and LEM-2 is present in the peripheral ER throughout the cell cycle. Table S1 lists the putative Rab-type GTPases in *C. elegans*. Table S2 lists the strains used in this study. Table S3 lists the dsRNAs used in this study. Video 1 shows the ER morphology in embryos depleted of RAB-5 or YOP-1/RET-1. Video 2 shows that RAB-5 is required for ER structure and dynamics. Video 3 shows that expression of activated $RAB\text{-}5^{Q78L}$ potentiates ER clustering. Video 4 shows that codepletion of RAB-5 and YOP-1/RET-1 leads to a synergistic defect in ER morphology. Video 5 shows that RAB-5 depletion blocks nuclear envelope disassembly. Online supplemental material is available at http://www.jcb.org/cgi/content/full/jcb.200701139/DC1.

We thank Gary Bokoch, William Balch, Marino Zerial, Jennifer Lippincott-Schwartz, Barth Grant, and Peter Askjaer for strains and reagents. Some nematode strains used in this work were provided by the Caenorhabditis Genetics Center, which is funded by the National Institutes of Health National Center for Research Resources (NCRR).

A. Audhya is a fellow of the Helen Hay Whitney Foundation; K. Oegema is a Pew Scholar in the Biomedical Sciences; A. Desai is the Connie and Bob Lurie Scholar of the Damon Runyon Cancer Research Foundation (DRS 38-04). K. Oegema and A. Desai receive salary and additional support from the Ludwig Institute for Cancer Research.

Submitted: 25 January 2007
Accepted: 31 May 2007

References

Audhya, A., F. Hyndman, I.X. McLeod, A.S. Maddox, J.R. Yates III, A. Desai, and K. Oegema. 2005. A complex containing the Sm protein CAR-1 and the RNA helicase CGH-1 is required for embryonic cytokinesis in *Caenorhabditis elegans*. *J. Cell Biol.* 171:267–279.

Baumann, O., and B. Walz. 2001. Endoplasmic reticulum of animal cells and its organization into structural and functional domains. *Int. Rev. Cytol.* 205:149–214.

Bobinnec, Y., C. Marcaillou, X. Morin, and A. Debec. 2003. Dynamics of the endoplasmic reticulum during early development of *Drosophila melanogaster*. *Cell Motil. Cytoskeleton.* 54:217–225.

Calero, M., G.R. Whittaker, and R.N. Collins. 2001. Yop1p, the yeast homolog of the polyposis locus protein 1, interacts with Yip1p and negatively regulates cell growth. *J. Biol. Chem.* 276:12100–12112.

Cheeseman, I.M., S. Niessen, S. Anderson, F. Hyndman, J.R. Yates III, K. Oegema, and A. Desai. 2004. A conserved protein network controls assembly of the outer kinetochore and its ability to sustain tension. *Genes Dev.* 18:2255–2268.

Christoforidis, S., H.M. McBride, R.D. Burgoyne, and M. Zerial. 1999. The Rab5 effector EEA1 is a core component of endosome docking. *Nature.* 397:621–625.

Cole, N.B., C.L. Smith, N. Sciaky, M. Terasaki, M. Edidin, and J. Lippincott-Schwartz. 1996. Diffusional mobility of Golgi proteins in membranes of living cells. *Science.* 273:797–801.

De Craene, J.O., J. Coleman, P. Estrada de Martin, M. Pypaert, S. Anderson, J.R. Yates III, S. Ferro-Novick, and P. Novick. 2006. Rtn1p is involved in structuring the cortical endoplasmic reticulum. *Mol. Biol. Cell.* 17:3009–3020.

Deneka, M., M. Neeft, and P. van der Sluijs. 2003. Regulation of membrane transport by rab GTPases. *Crit. Rev. Biochem. Mol. Biol.* 38:121–142.

Desai, A., S. Rybina, T. Muller-Reichert, A. Shevchenko, A. Hyman, and K. Oegema. 2003. KNL-1 directs assembly of the microtubule-binding interface of the kinetochore in *C. elegans*. *Genes Dev.* 17:2421–2435.

D'Hondt, K., A. Heese-Peck, and H. Riezman. 2000. Protein and lipid requirements for endocytosis. *Annu. Rev. Genet.* 34:255–295.

Dreier, L., and T.A. Rapoport. 2000. In vitro formation of the endoplasmic reticulum occurs independently of microtubules by a controlled fusion reaction. *J. Cell Biol.* 148:883–898.

Du, Y., S. Ferro-Novick, and P. Novick. 2004. Dynamics and inheritance of the endoplasmic reticulum. *J. Cell Sci.* 117:2871–2878.

Dunn, W.A., Jr. 1990. Studies on the mechanisms of autophagy: formation of the autophagic vacuole. *J. Cell Biol.* 110:1923–1933.

Ellenberg, J., E.D. Siggia, J.E. Moreira, C.L. Smith, J.F. Presley, H.J. Worman, and J. Lippincott-Schwartz. 1997. Nuclear membrane dynamics and reassembly in living cells: targeting of an inner nuclear membrane protein in interphase and mitosis. *J. Cell Biol.* 138:1193–1206.

Estrada de Martin, P., P. Novick, and S. Ferro-Novick. 2005. The organization, structure, and inheritance of the ER in higher and lower eukaryotes. *Biochem. Cell Biol.* 83:752–761.

Franz, C., P. Askjaer, W. Antonin, C.L. Iglesias, U. Haselmann, M. Schelder, A. de Marco, M. Wilm, C. Antony, and I.W. Mattaj. 2005. Nup155 regulates nuclear envelope and nuclear pore complex formation in nematodes and vertebrates. *EMBO J.* 24:3519–3531.

Galy, V., I.W. Mattaj, and P. Askjaer. 2003. Caenorhabditis elegans nucleoporins Nup93 and Nup205 determine the limit of nuclear pore complex size exclusion in vivo. *Mol. Biol. Cell.* 14:5104–5115.

Gerace, L., and B. Burke. 1988. Functional organization of the nuclear envelope. *Annu. Rev. Cell Biol.* 4:335–374.

Grant, B., and D. Hirsh. 1999. Receptor-mediated endocytosis in the *Caenorhabditis elegans* oocyte. *Mol. Biol. Cell.* 10:4311–4326.

Gruenbaum, Y., A. Margalit, R.D. Goldman, D.K. Shumaker, and K.L. Wilson. 2005. The nuclear lamina comes of age. *Nat. Rev. Mol. Cell Biol.* 6:21–31.

Hetzer, M., D. Bilbao-Cortes, T.C. Walther, O.J. Gruss, and I.W. Mattaj. 2000. GTP hydrolysis by Ran is required for nuclear envelope assembly. *Mol. Cell.* 5:1013–1024.

Hetzer, M.W., T.C. Walther, and I.W. Mattaj. 2005. Pushing the envelope: structure, function, and dynamics of the nuclear periphery. *Annu. Rev. Cell Dev. Biol.* 21:347–380.

Holaska, J.M., K.L. Wilson, and M. Mansharamani. 2002. The nuclear envelope, lamins and nuclear assembly. *Curr. Opin. Cell Biol.* 14:357–364.

Holmer, L., and H.J. Worman. 2001. Inner nuclear membrane proteins: functions and targeting. *Cell. Mol. Life Sci.* 58:1741–1747.

King, M.C., C.P. Lusk, and G. Blobel. 2006. Karyopherin-mediated import of integral inner nuclear membrane proteins. *Nature.* 442:1003–1007.

Kline, D. 2000. Attributes and dynamics of the endoplasmic reticulum in mammalian eggs. *Curr. Top. Dev. Biol.* 50:125–154.

Klionsky, D.J., and S.D. Emr. 2000. Autophagy as a regulated pathway of cellular degradation. *Science.* 290:1717–1721.

Lee, C., and L.B. Chen. 1988. Dynamic behavior of endoplasmic reticulum in living cells. *Cell.* 54:37–46.

Lenart, P., G. Rabut, N. Daigle, A.R. Hand, M. Terasaki, and J. Ellenberg. 2003. Nuclear envelope breakdown in starfish oocytes proceeds by partial NPC disassembly followed by a rapidly spreading fenestration of nuclear membranes. *J. Cell Biol.* 160:1055–1068.

Maddox, P.S., N. Portier, A. Desai, and K. Oegema. 2006. Molecular analysis of mitotic chromosome condensation using a quantitative time-resolved fluorescence microscopy assay. *Proc. Natl. Acad. Sci. USA.* 103:15097–15102.

Margalit, A., S. Vlcek, Y. Gruenbaum, and R. Foisner. 2005. Breaking and making of the nuclear envelope. *J. Cell. Biochem.* 95:454–465.

Mattaj, I.W. 2004. Sorting out the nuclear envelope from the endoplasmic reticulum. *Nat. Rev. Mol. Cell Biol.* 5:65–69.

McNally, K., A. Audhya, K. Oegema, and F.J. McNally. 2006. Katanin controls mitotic and meiotic spindle length. *J. Cell Biol.* 175:881–891.

Motegi, F., N.V. Velarde, F. Piano, and A. Sugimoto. 2006. Two phases of astral microtubule activity during cytokinesis in *C. elegans* embryos. *Dev. Cell.* 10:509–520.

Munafo, D.B., and M.I. Colombo. 2002. Induction of autophagy causes dramatic changes in the subcellular distribution of GFP-Rab24. *Traffic.* 3:472–482.

Nance, J., E.M. Munro, and J.R. Priess. 2003. *C. elegans* PAR-3 and PAR-6 are required for apicobasal asymmetries associated with cell adhesion and gastrulation. *Development.* 130:5339–5350.

Oegema, K., and A.A. Hyman. 2005. Cell division. In WormBook, editors. Available at: http://www.wormbook.org (accessed June 15, 2005).

Oegema, K., A. Desai, S. Rybina, M. Kirkham, and A.A. Hyman. 2001. Functional analysis of kinetochore assembly in *Caenorhabditis elegans*. *J. Cell Biol.* 153:1209–1226.

Ohba, T., E.C. Schirmer, T. Nishimoto, and L. Gerace. 2004. Energy- and temperature-dependent transport of integral proteins to the inner nuclear membrane via the nuclear pore. *J. Cell Biol.* 167:1051–1062.

Palade, G.E. 1955. Studies on the endoplasmic reticulum. II. Simple dispositions in cells in situ. *J. Biophys. Biochem. Cytol.* 1:567–582.

Papp, S., E. Dziak, M. Michalak, and M. Opas. 2003. Is all of the endoplasmic reticulum created equal? The effects of the heterogeneous distribution of endoplasmic reticulum Ca^{2+}-handling proteins. *J. Cell Biol.* 160:475–479.

Pfeffer, S.R. 2001. Rab GTPases: specifying and deciphering organelle identity and function. *Trends Cell Biol.* 11:487–491.

Portier, N., A. Audhya, P.S. Maddox, R.A. Green, A. Dammermann, A. Desai, and K. Oegema. 2007. A microtubule-independent role for centrosomes and Aurora A in nuclear envelope breakdown. *Dev. Cell.* 12:515–529.

Poteryaev, D., J.M. Squirrell, J.M. Campbell, J.G. White, and A. Spang. 2005. Involvement of the actin cytoskeleton and homotypic membrane fusion in ER dynamics in *Caenorhabditis elegans*. *Mol. Biol. Cell.* 16:2139–2153.

Praitis, V., E. Casey, D. Collar, and J. Austin. 2001. Creation of low-copy integrated transgenic lines in *Caenorhabditis elegans*. *Genetics.* 157:1217–1226.

Prunuske, A.J., and K.S. Ullman. 2006. The nuclear envelope: form and reformation. *Curr. Opin. Cell Biol.* 18:108–116.

Salina, D., K. Bodoor, P. Enarson, W.H. Raharjo, and B. Burke. 2001. Nuclear envelope dynamics. *Biochem. Cell Biol.* 79:533–542.

Sato, K., M. Sato, A. Audhya, K. Oegema, P. Schweinsberg, and B.D. Grant. 2006. Dynamic regulation of caveolin-1 trafficking in the germ line and embryo of *Caenorhabditis elegans*. *Mol. Biol. Cell.* 17:3085–3094.

Sato, M., K. Sato, P. Fonarev, C. Huang, W. Liou, and B.D. Grant. 2005. *Caenorhabditis elegans* RME-6, a novel regulator of Rab5 at the clathrin-coated pit. *Nat. Cell Biol.* 7:559–569.

Shibata, Y., G.K. Voeltz, and T.A. Rapoport. 2006. Rough sheets and smooth tubules. *Cell.* 126:435–439.

Somsel Rodman, J., and A. Wandinger-Ness. 2000. Rab GTPases coordinate endocytosis. *J. Cell Sci.* 113:183–192.

Sönnichsen, B., L.B. Koski, A. Walsh, P. Marschall, B. Neumann, M. Brehm, A.M. Alleaume, J. Artelt, P. Bettencourt, E. Cassin, et al. 2005. Full-genome RNAi profiling of early embryogenesis in *Caenorhabditis elegans*. *Nature.* 434:462–469.

Soullam, B., and H.J. Worman. 1995. Signals and structural features involved in integral membrane protein targeting to the inner nuclear membrane. *J. Cell Biol.* 130:15–27.

Stricker, S.A. 2006. Structural reorganizations of the endoplasmic reticulum during egg maturation and fertilization. *Semin. Cell Dev. Biol.* 17:303–313.

Terasaki, M. 2000. Dynamics of the endoplasmic reticulum and Golgi apparatus during early sea urchin development. *Mol. Biol. Cell.* 11:897–914.

Terasaki, M., and L.A. Jaffe. 1991. Organization of the sea urchin egg endoplasmic reticulum and its reorganization at fertilization. *J. Cell Biol.* 114:929–940.

Terasaki, M., L.L. Runft, and A.R. Hand. 2001. Changes in organization of the endoplasmic reticulum during *Xenopus* oocyte maturation and activation. *Mol. Biol. Cell.* 12:1103–1116.

Tran, E.J., and S.R. Wente. 2006. Dynamic nuclear pore complexes: life on the edge. *Cell.* 125:1041–1053.

Turner, M.D., H. Plutner, and W.E. Balch. 1997. A Rab GTPase is required for homotypic assembly of the endoplasmic reticulum. *J. Biol. Chem.* 272:13479–13483.

Vedrenne, C., and H.P. Hauri. 2006. Morphogenesis of the endoplasmic reticulum: beyond active membrane expansion. *Traffic.* 7:639–646.

Voeltz, G.K., M.M. Rolls, and T.A. Rapoport. 2002. Structural organization of the endoplasmic reticulum. *EMBO Rep.* 3:944–950.

Voeltz, G.K., W.A. Prinz, Y. Shibata, J.M. Rist, and T.A. Rapoport. 2006. A class of membrane proteins shaping the tubular endoplasmic reticulum. *Cell.* 124:573–586.

Waterman-Storer, C.M., and E.D. Salmon. 1998. Endoplasmic reticulum membrane tubules are distributed by microtubules in living cells using three distinct mechanisms. *Curr. Biol.* 8:798–806.

Watson, M.L. 1955. The nuclear envelope; its structure and relation to cytoplasmic membranes. *J. Biophys. Biochem. Cytol.* 1:257–270.

Yang, L., T. Guan, and L. Gerace. 1997. Integral membrane proteins of the nuclear envelope are dispersed throughout the endoplasmic reticulum during mitosis. *J. Cell Biol.* 137:1199–1210.

Zerial, M., and H. McBride. 2001. Rab proteins as membrane organizers. *Nat. Rev. Mol. Cell Biol.* 2:107–117.